ACS APPLIED MATERIALS & INTERFACES

Research Article

www.acsami.org

Colorimetric Au Nanoparticle Probe for Speciation Test of Arsenite and Arsenate Inspired by Selective Interaction between Phosphonium Ionic Liquid and Arsenite

Zhi-Qiang Tan, Jing-Fu Liu,* Yong-Guang Yin, Qian-Tao Shi, Chuan-Yong Jing, and Gui-Bin Jiang

State Key Laboratory of Environmental Chemistry and Ecotoxicology, Research Center for Eco-Environmental Sciences, Chinese Academy of Sciences, Beijing 100085, China

Ⓢ *Supporting Information*

ABSTRACT: The exposure of millions of people to unsafe levels of arsenite (As^{III}) and arsenate (As^{V}) in drinking waters calls for the development of low-cost methods for on-site monitoring these two arsenic species in waters. Herein, for the first time, tetradecyl (trihexyl) phosphonium chloride ionic liquid was found to selectively bind with As^{III} via extended X-ray absorption fine structure (EXAFS) analysis. Based on the finding, an As^{III}-specific probe was developed by modifying gold nanoparticles with the ionic liquid. Futhermore, Hofmeister effect was primarily observed to significantly affect the sensitivity of gold nanoparticle probe. With the colorimetric probe, we developed a protocol for naked eye speciation test of As^{III} and As^{V} at levels below the World Health Organization (WHO) guideline of 10 μg L^{-1}. This method featured with high tolerance to common coexisting ions such as 10 mM PO_4^{3-}, and was validated by assaying certified reference and environmental water samples.

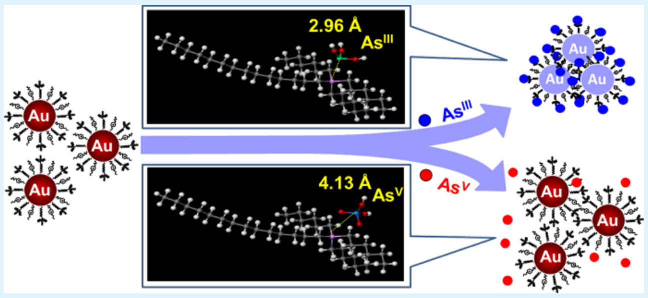

KEYWORDS: *arsenic, ionic liquid, interaction, gold nanoparticle, Hofmeister effect, visual test*

■ INTRODUCTION

Arsenic shows various adverse health effects including carcinogenic disease relative to skin, lung, and kidney.[1−3] More than 140 million people worldwide are exposed to superfluous arsenic, mainly by drinking ground waters polluted by inorganic arsenic that are more toxic than the organic ones.[4,5] Although As^{III} and As^{V} are coexisting and undergo mutual transformation in groundwater, As^{III} is usually the main form and more toxic than As^{V}.[6] Consequently, monitoring of inorganic arsenic species in waters is of prior interest in arsenic detection. Numerous instrumental methods have been developed to quantify trace arsenic,[7−10] but the requirement of bulk equipment and strict laboratory conditions restricts their application in field analysis. On the contrary, the colorimetric or visual methods are quite suitable for field determination. Because of their poor sensitivity, however, traditional visual probes are incapable of detecting As^{III} and As^{V} at 10 μg L^{-1} level, which is the arsenic guideline value in drinking water required by the World Health Organization (WHO) and U.S. Environmental Protection Agency (EPA). Additionally, the fairly poor tolerance to interferences of these probes restricts their application in real sample analysis.[11−13] Several arsenic testing field kits are able to semiquantify 10 or 50 μg L^{-1} As, but most of them fail to meet the requirements of an ideal test kit for As.[14−16]

Gold nanoparticles (AuNPs) are widely used as optical probes in colorimetric detection in recent years,[17−19] because of their higher extinction coefficient in the visible region and thus higher sensitivity in comparison to the organic probes. Since the pioneering work of the Mirkin group,[20] AuNPs have served as optical probes for sensing cations, anions, small organic compounds, and biological molecules,[21−23] with Hg^{2+} as one of the most attractive target analytes.[24−31] Surprisingly, studies on the use of AuNPs as optical probes to detect arsenic are sparse.[32,33] By successively modifying the surface of AuNPs with glutathione, dithiothreitol and cysteine, Ray's group developed a label-free optical probe for colorimetric detection of arsenic at μg L^{-1} level by naked eyes.[32] In that procedure, the total amount of As^{III} and As^{V} was quantified because As^{V} was inevitably reduced to As^{III} by dithiothreitol, which was used as an essential modifier. To the best of our knowledge, speciation test of inorganic As^{III} and As^{V} with a single AuNP probe has not been reported yet, and it remains a great challenge to test the two inorganic arsenic species at low μg L^{-1} levels with naked eyes.

Herein, a phosphonium ionic liquid, tetradecyl trihexyl phosphonium chloride ($[C_{14}(C_6)_3P]Cl$) (P-IL), was first found to have strong interaction with As^{III}, which was verified by extended X-ray absorption fine structure (EXAFS) analysis. Modified with the ionic liquid, an efficient gold nanoparticle

Received: August 4, 2014
Accepted: October 21, 2014
Published: October 21, 2014

probe was developed and applied to achieve visual speciation test of As^{III} and As^{V} with high selectivity and sensitivity. As described in Scheme 1, As^{III} is detected directly based on the color-changing of the probe from red to blue. The total amount of inorganic As is detected by prereducing As^{V} into As^{III} with ascorbic acid, and As^{V} level is determined indirectly by substrating As^{III} from the total inorganic As. On the basis of the procedure proposed, this $C_{14}(C_6)_3P^+$-modified AuNP (P-AuNPs) was applied to determine both As^{III} and As^{V} concentration in water samples at the μg L^{-1}.

Scheme 1. Schematic Representation of the Mechanism of P-AuNPs for Determination of As^{III} and As^{V}

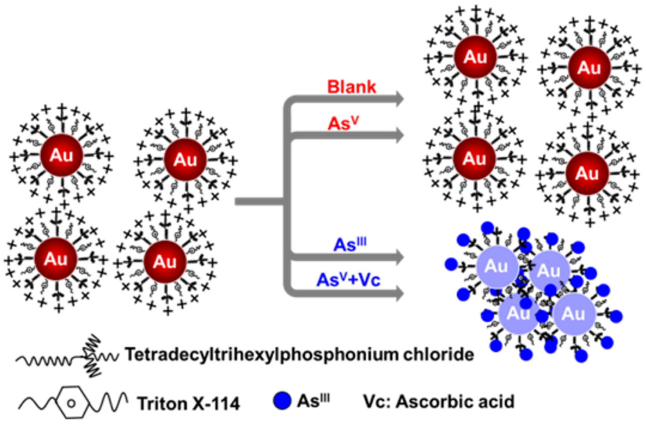

EXPERIMENTAL SECTION

Chemicals and Equipment. Standard stock solutions of As^{III} (GBW08666) and As^{V} (GBW08667) were obtained from the National Institute of Metrology (China). $[C_{14}(C_6)_3P]Cl$ (Cyphos IL-101) was purchased from Sigma-Aldrich (St. Louis, MO, USA). Triton X-114 (TX-114) was got from Acros Organics (Geel, Belgium). Potassium borohydride was obtained from Tianjin Jinke Fine Chemical Institute (Tianjin, China). All the other chemicals were from Sinopharm Chemical Reagent Co. (Beijing, China) with purity of at least of analytical grade and were used without further purification. Ultrapure water (18.3 MΩ) from a Milli-Q Gradient system (Millipore, Bedford) was used throughout the whole study. The certified reference arsenic water sample (GBW08605) was obtained from National Institute of Metrology (China). The lake water was collected from a local water source reserve (Changbaishan, China). The groundwater was obtained from a village in Datong, Shanxi Province (China), which was reported to have been contaminated by arsenic.[34]

A pH meter (Orion, Thermo) was used to adjust the acidity of buffer solutions. P-AuNPs were characterized by transmission electron microscope (TEM) (H7500, Hitachi). A multimode microplate spectrophotometer (Varioscan Flash, Thermo) was adopted to record absorbance in the range of 400−800 nm. As EXAFS spectra were collected at beamline 01C1 in the National Synchrotron Radiation Research Center, Taiwan. High performance liquid chromatography (HPLC) (1200, Agilent) and an atomic fluorescence spectrometer (AFS) (8130, Titan, China) were hyphenated by a homemade connector for studying conversion reaction of As^{III} to As^{V}. A guard column (25 mm × 2.3 mm, 12−20 μm) was used for in-line cleanup the P-AuNPs in the test solutions. Chromatographic separation of As^{III} and As^{V} was carried out on a Hamilton PRP-X100 column (250 mm × 4.1 mm, 10 μm), with phosphate buffer (5 mM) as mobile phase set at a flow rate of 1 mL min^{-1}.

Synthesis of Phosphonium Ionic Liquid-Functionalized Gold Nanoparticles. P-AuNPs were prepared by reduction of $HAuCl_4$ with KBH_4 in the presence of $[C_{14}(C_6)_3P]Cl$.[35] Briefly, into 10 mL of an aqueous solution, containing ionic liquid (5 mg) and Triton X-114 (2 mg), was added 200 μL $HAuCl_4$ (1%). After stirring for 10 min, 10 mL of KBH_4 (1.1 mg) was added dropwise into the mixture. After stirring another 10 min, the mixture displayed wine red in color indicating formation of P-AuNPs. The unreacted reagents were discarded through centrifugation (17000 × g, 15 min). The concentration of P-AuNPs estimated from Beer's law was 3 nM,[25] and the P-AuNP stock solution was prepared by diluting the concentrated P-AuNPs at the bottom of centrifuge tubes to the original volume.

Speciation Test of As^{III} and As^{V} with P-AuNPs as a Colorimetric Probe. For detection of As^{III}, into a 200 μL polyethylene vial or a well of the 96 well-plate was added 50 μL of the standard or sample solutions, 50 μL of NH_4NO_3−$NH_3{\cdot}H_2O$ buffer solutions (0.03 M, pH 10.2), and 50 μL of P-AuNP stock solution (3 nM). After incubation for 30 min at room temperature visual or colorimetric detection was conducted. For speciation test, 0.01 mM ascorbic acid was additionally added into the mixture solutions above to reduce As^{V} to As^{III}. The amount of As^{V} was quantified indirectly by

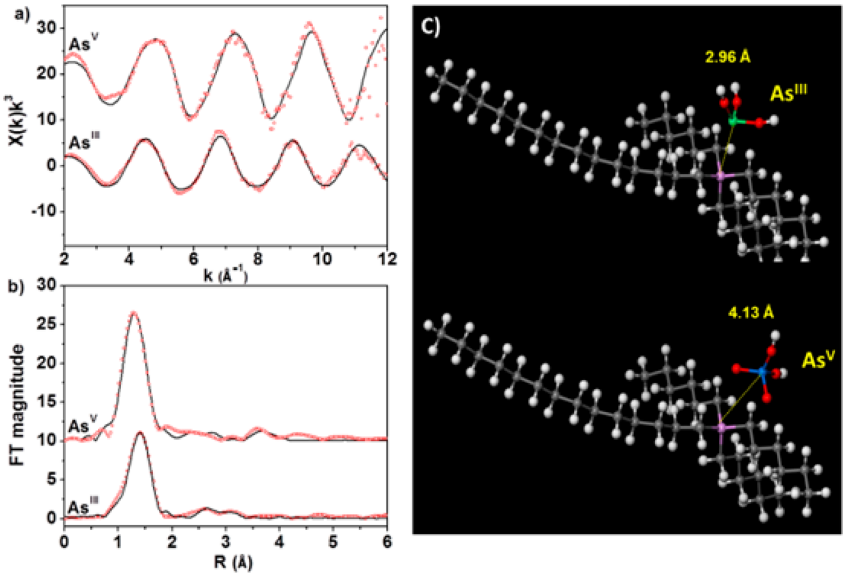

Figure 1. (a) EXAFS spectra (solid lines) and shell fits (open dots) of As^{III} and As^{V} solutions with $[C_{14}(C_6)_3P]Cl$ (pH 10.2); (b) Fourier transform magnitudes (solid lines) and shell fits (open dots); (c) simulated molecular structures of $C_{14}(C_6)_3P^+$-$H_2AsO_3^-$ and $C_{14}(C_6)_3P^+$-$HAsO_4^{2-}$.

the difference between the total inorganic As and As^{III}. The multimode microplate spectrophotometer with a 96 well-plate was employed for recording the absorbance value.

■ RESULTS AND DISCUSSION

Selective Interaction between Tetradecyl Trihexyl Phosphonium and As^{III}. According to the principle of "like dissolves like", as well as the successes in extraction of neutral form of arsenic with phosphine derivatives[36−39] and As^V-molybdate heteropoly acid with phosphonium,[40] the P-ILs may own strong interaction with arsenic species. To verify this, we applied EXAFS to determine the association of $C_{14}(C_6)_3P^+$ with As ions in aqueous solutions at pH 10.2. The k^3-weighted As K-edge EXAFS spectra, the corresponding radial structure functions (RSF) as magnitude of the Fourier transformation (FT) versus radial distance are shown in Figure 1a, b. The optimal parameters listed in Table 1 were obtained by fitting the theoretical curves to the experimental spectra. The FT of EXAFS spectra was able to isolate the contributions of different coordination shells, in which the peak positions corresponded to the interatomic distances. It is noteworthy that these peak positions are shifted from the true distance by 0.3−0.5 Å as they were uncorrected for phase shift. According to the fit of the theoretical to the experimental spectra, the first and strongest peak in the FT curve was contributable to 3 oxygen atoms at an average distance of 1.79 Å for $C_{14}(C_6)_3P-As^{III}$ and 4 oxygen atoms at an average distance of 1.69 Å for $C_{14}(C_6)_3P-As^V$, respectively. The distances of $As^{III}-O$ and As^V-O are in good agreement with previously published data.[41,42] Furthermore, the P atoms were detected at 2.96 Å with a coordination number (CN) of 1.07 for $C_{14}(C_6)_3P-As^{III}$, and at 4.13 Å with CN of 0.84 for $C_{14}(C_6)_3P-As^V$ (Figure 1c), indicating that both As^{III} and As^V are associated with $C_{14}(C_6)_3P^+$ via the As−O−P bonding, but the bonding of $C_{14}(C_6)_3P^+$ to $H_2AsO_3^-$ is much stronger than that to $HAsO_4^{2-}$.

Table 1. Structural Characterization of As^{III} and As^V in the Water Samples Containing $[C_{14}(C_6)_3P]Cl$ by Shell Fitting in r-Space Using Theoretical Paths

sample	shell	CN[a]	R^b (Å)	σ^{2c} (Å^2)	$\Delta E_0{}^d$ (eV)
$As^{III}-P$	As−O	3 (set)	1.79 ± 0.01	0.001	11.74
	As−P	0.97 ± 0.13	2.96 ± 0.03	0.001	
As^V-P	As−O	4 (set)	1.69 ± 0.01	0.001	6.68
	As−P	0.84 ± 0.28	4.13 ± 0.06	0.005	

[a] Coordination number. [b] Interatomic distance. [c] Debye−Waller factor. [d] Threshold energy shift.

Selection of P-IL as Modifier for As^{III}−Specific Probe. Besides for the selective interaction between P-IL and As^{III}, P-ILs with unique properties[43−45] should have great potentials in functionalizing AuNPs, because cationic surfactant properties of P-ILs with long chain make them ideal coating agents for stabilizing the AuNPs. To verify this, we modified ∼11 nm AuNPs, the most commonly used one in AuNP probe preparation, with tetrabutyl phosphonium bromide ($[(C_4)_4P]Br$), dodecyl tributyl phosphonium bromide ($[C_{12}(C_4)_3P]Br$), and tetradecyl trihexyl phosphonium chloride ($[C_{14}(C_6)_3P]Cl$). For comparison, another two water-soluble ILs, including hexadecyl trimethylammonium bromide and 1-hexadecyl-3-methylimidazolium chloride, were as well-employed as the modifier. The modification was conducted simultaneously in the preparation process of 11 nm AuNPs according to a previously reported method.[35] Results showed that only the 3 phosphonium-based ILs gave rise to relatively stable AuNPs, among which only the $C_{12}(C_4)_3P^+$ or $C_{14}(C_6)_3P^+$-modified AuNPs showed a color-changing from red to blue in the presence of As^{III}. In addition, the AuNP modified with $C_{14}(C_6)_3P^+$ is relatively more stable and sensitive to As^{III} than that with $C_{12}(C_4)_3P^+$, possibly because of the relatively longer alkyl chains of $C_{14}(C_6)_3P^+$. Unfortunately, even this $C_{14}(C_6)_3P^+$ modified AuNPs (P-AuNPs) is not stable enough in media with relatively high ionic strength, which limits its application in real samples. To further improve the probe stability, neutral nonionic surfactants Triton X-114, which shows great potential in stabilizing nanomaterials,[46] was introduced as the coating agent. This coating agent largely improved the stability of AuNPs, which remain well-dispersed in the $NH_4NO_3-NH_3 \cdot H_2O$ buffer up to 15 mM, and markedly enhanced the probe stability in real water samples without reduction of probe sensitivity to As^{III}. Therefore, $[C_{14}(C_6)_3P]Cl$ was selected as the suitable modifier in preparation of P-AuNPs. The P-AuNPs were characterized by transmission electron microscopy (TEM) with the average size of 11.1 nm (see Figure S1 in the Supporting Information).

Specificity of P-AuNP to As^{III}. Very importantly, the P-AuNP probe shows extremely high specificity to As^{III}. In comparison to As^V, As^{III} gave rise to much more significant color change of the test solution from red to purple or blue, which was represented by the increment of ratio of absorption at 630 nm to that at 525 nm ($\Delta(A_{630}/A_{525})$), especially at pH 10.2 the $\Delta(A_{630}/A_{525})$ induced by As^{III} is ∼10 times of that by As^V (Figure 2a). To understand the specific response of the probe to As^{III}, we respectively measured the zeta potentials of P-AuNP probe alone and its respective mixture with As^{III} and As^V at various pHs. Results shown in Figure 2b indicate that in

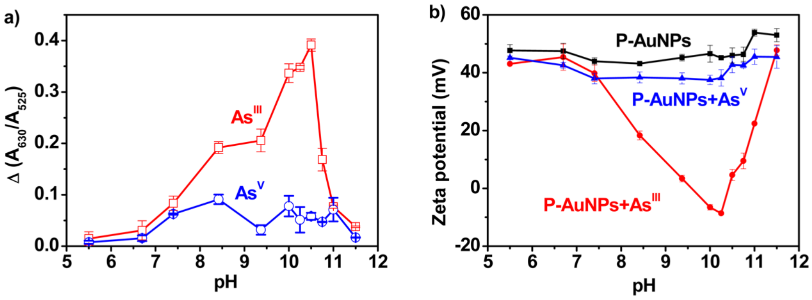

Figure 2. (a) Effect of pH on the absorption ratio change ($\Delta(A_{630}/A_{525})$) of P-AuNPs in the presence of As^{III} or As^{III}; (b) zeta potentials of P-AuNPs, P-AuNPs + As^{III}, and P-AuNPs + As^V at different pH values. The respective concentrations of As^{III} and As^V are 15 μg L^{-1}.

the presence of As^V, the zeta potential of the P-AuNP probe kept almost constant in the entire studied pH range, which is similar to that in blank solution. In the presence of As^{III}, however, the zeta potential of the P-AuNP probe markedly decreased at pH 8.0−11.0, thus the solutions appear purple or blue because of the probe aggregation, which was evidenced by the transmission electron microscope (TEM) image. As shown in Figure 3a, the TEM iamges revealed P-AuNPs still kept well disperse in the NH_4NO_3−$NH_3 \cdot H_2O$ buffer solution. However, in the presence of As^{III} and the buffer solution, aggregation of P-AuNPs was observed (Figure 3b). This suggests that As^{III} (pK_a 12.1, ~90% in the form of $H_2AsO_3^-$ at pH 10.2[47−49]) strongly associated with $C_{14}(C_6)_3P^+$, whereas As^V (pK_a 6.9, ~95% in the form of $HAsO_4^{2-}$ at pH 10.2[47−49]) has negligible association with $C_{14}(C_6)_3P^+$. The strong association between $H_2AsO_3^-$ and $C_{14}(C_6)_3P^+$ agreed with a previous report,[50] in which $C_{14}(C_6)_3P^+$ was assumed to react with $HCrO_4^-$ to form $[C_{14}(C_6)_3P]HCrO_4$ through anion exchange.

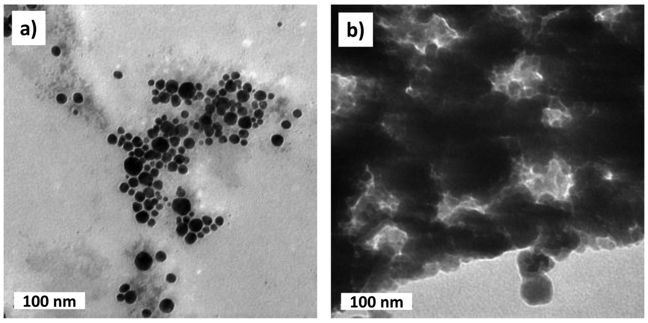

Figure 3. TEM images of P-AuNPs after mixing with (a) buffer solution, (b) buffer solution and As^{III}. Buffer solution: pH 10.2, NH_4NO_3−$NH_3 \cdot H_2O$, 10 mM; As^{III}: 15 μg L^{-1}.

Optimization of the Chromogenic Assay. In view of the strong dependence of arsenic species on pH and the instability of AuNPs in strong acid or basic media, the method sensitivity is highly dependent on the solution pH (Figure 2a). While the increase of response (Δ (A_{630}/A_{525})) with pH in the range of 5.5−10.2 can be ascribed to the increase of $H_2AsO_3^-$ fraction, the dramatic dropping of the $\Delta(A_{630}/A_{525})$ value in pH 10.5−11.0 is out of our expectation, as $H_2AsO_3^-$ is still the dominant form of As^{III} in this pH range. We speculate that As^{III} was partly oxidized to As^V, which therefore reduced the response. To verify this, we studied the conversion of As^{III} to As^V with HPLC-AFS. Results showed that the P-AuNPs and solution pH play a major role in the oxidization of As^{III} (see Figure S2 in the Supporting Information). Without P-AuNPs, no oxidization of As^{III} occurred in 90 min at both pH 10.2 and pH 11.0, whereas the oxidization of As^{III} to As^V gradually reached to ~65% (pH 11.0) and ~30% (pH 10.2), respectively, when the reaction time extended to 500 min. However, the presence of P-AuNPs markedly enhanced the oxidization kinetics of As^{III} to As^V, with a half-life period of about 50 min (pH 11.0) and 120 min (pH 10.2) for As^{III}, and an oxidization ratio of ~100% (pH 11.0) and ~90% (pH 10.2) at 500 min, respectively. The enhanced oxidization of As^{III} suggests that P-AuNPs can catalyze this reaction and alleviate the As toxicity to some extent, and further study is being conducted in our laboratory.

The effect of buffer species was further evaluated by comparison to Tris and phosphate buffer, respectively, and it was demonstrated that ammonia-based buffers provided superiority in sensitivity and rapidity primarily as a result of strong Hofmeister effect. Interestingly, the method sensitivity is strongly dependent on the species of ammonium salts used together with $NH_3 \cdot H_2O$ for preparing the buffer solutions. Six ammonium salts including NH_4SCN, NH_4NO_3, NH_4Cl, $NH_4H_2PO_4$, $(NH_4)_2SO_4$, and CH_3COONH_4 were tested, and it was only in NH_4SCN-$NH_3 \cdot H_2O$ and NH_4NO_3−$NH_3 \cdot H_2O$ buffer that the P-AuNPs showed response to As^{III}, possibly because of the strong Hofmeister effect of SCN^- and NO_3^-,[51] and therefore lead to enhanced aggregation of the P-AuNPs. However, the Hofmeister effect of SCN^- was so strong that it induced significant blank response of the P-AuNP probe, thus NH_4NO_3−$NH_3 \cdot H_2O$ buffer was selected in the following experiments. The buffer concentration also significantly affects the response of the P-AuNP probe to As^{III} (Figure 4), and the highest sensitivity was obtained in 10−15 mM NH_4NO_3−$NH_3 \cdot H_2O$ buffer solutions. Lower buffer concentration is unfavorable to control the optimum pH value (pH 10.2), whereas higher buffer concentration could enhance the blank response due to the salt effect.

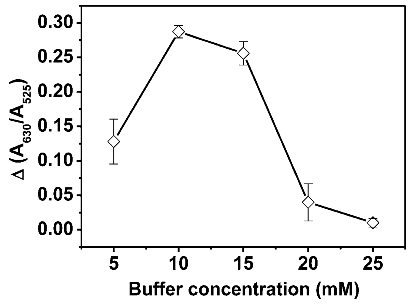

Figure 4. Effect of buffer concentration on the absorption ratio change ($\Delta(A_{630}/A_{525})$) of P-AuNPs in the presence of 15 μg L^{-1} As^{III}.

It is well-known that the AuNP probe concentration has significant effect on the detection sensitivity.[24−27] Small amount of P-AuNPs are not able to react with As^{III} completely, while more P-AuNPs lead to higher blank absorbance. Both of the aforementioned conditions give rise to low sensitivity. Here we optimized the probe concentration in the range of 0.25−1.5 nM, and 0.75 nM P-AuNPs gave rise to the maximum response to As^{III} (Figure 5).

Both colorimetric reaction temperature and time were further optimized to improve the detection. Although the response increased slightly with temperature from 4 to 37 °C and then decreased with the further increase in temperature (see Figure S3a in the Supporting Information), room

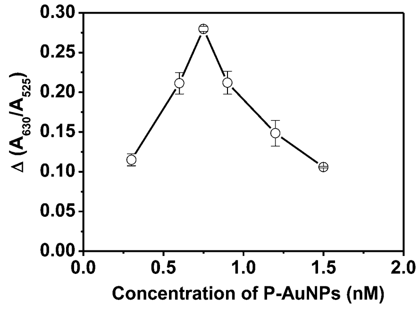

Figure 5. Effect of P-AuNPs concentration on the absorption ratio change ($\Delta(A_{630}/A_{525})$) of P-AuNPs in the presence of 15 μg L^{-1} As^{III}.

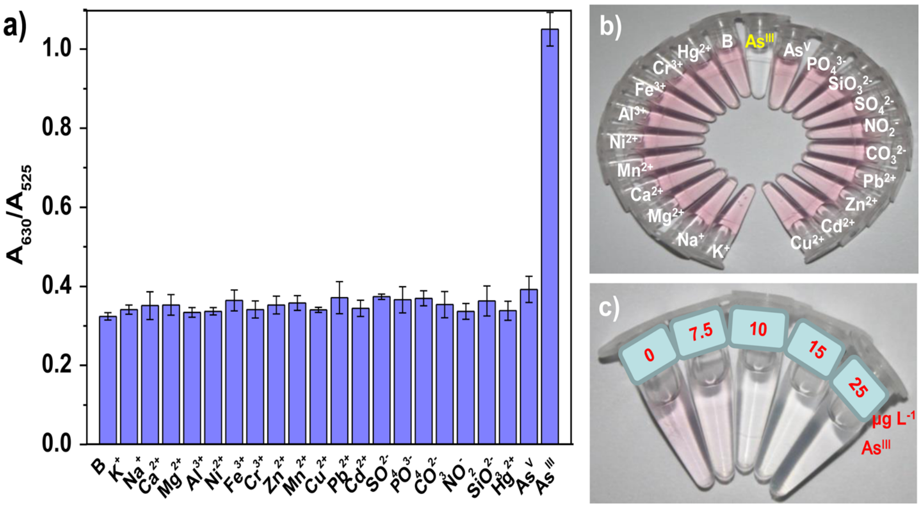

Figure 6. (a) Absorbance ratio (A_{630}/A_{525}) of P-AuNPs in the presence of As^{III}, As^{V}, and environmentally relevant ions; (b) photographic image of solutions of P-AuNPs containing common ions in the environment (As^{III}, 0.2 μM; other ions, 1 μM; B, blank); (c) Photographs of P-AuNPs solutions after addition of 0, 7.5, 10, 15, and 25 μg L^{-1} As^{III}.

temperature was adopted as it provides acceptable sensitivity and is more favorable for conduction. The response increased sharply with time up to 60 min and then almost level off (see Figure S3b in the Supporting Information), thus an incubation of 60 min can be used to achieve high sensitivity. However, in this work, an incubation period of 30 min, which provides half of the response at 60 min and satisfactory sensitivity, was adopted to reduce test time.

Analytical Performance. The selectivity of the proposed P-AuNP probe for As^{III} was evaluated by observing its responses to environmentally relevant cations (K^{+}, Na^{+}, Ca^{2+}, Mg^{2+}, Al^{3+}, Ni^{2+}, Fe^{3+}, Cr^{3+}, Zn^{2+}, Mn^{2+}, Pb^{2+}, Cd^{2+}, Hg^{2+}) and anions (SO$_4^{2-}$, PO$_4^{3-}$, CO$_3^{2-}$, NO$_2^{-}$, SiO$_3^{2-}$, As^{V}). Other common anions such as Cl^{-}, NO$_3^{-}$, and SCN^{-} were not tested, as experiments showed that the use of buffers containing high concentration of these anions had no interfere on the detection. As shown in Figure 6a and b, the probe had no response to at least 1.0 μM each of the other environmentally ions, whereas significant response to 0.2 μM As^{III} was observed. We also tested the interference from biomolecules and surfactants, and it was found that as high as 1% (m/v) sodium dodecyl sulfonate (SDS) and bovine serum albumin (BSA) showed no effect on the detection. When 0.01 mM ascorbic acid was introduced into the sample solutions to reduce As^{V} to As^{III}, the above results hold except that As^{V} showed the same response as that of As^{III} (see Figure S4 in the Supporting Information), again indicating the probe is applicable for speciation test of As^{III} and As^{V}. It is noteworthy that the P-AuNP probe can tolerate high concentration of PO$_4^{3-}$ (10 mM), which usually gives rise to significant interference in As detection by other probes.[13,52,53]

Next we studied the sensitivity of the proposed probe in the presence of different concentration of As^{III}. Under the above optimized conditions, the detection limit by naked eyes is 7.5 μg L^{-1} As^{III} (Figure 6c), which is lower than the limit of As for drinking water (10 μg L^{-1}) required by the World Health Organization and US EPA. Additionally, the repeatability evaluated by relative standard deviation (RSD) in measuring the $\Delta(A_{630}/A_{525})$ value of five standard solutions (10 μg L^{-1} As^{III}) with a UV–vis spectrophotometer was 5.9%. The same detection limit and repeatability were obtained for As^{V} after reduction with 0.01 mM ascorbic acid.

Practical Application. The applicability of the our novel nanoprobe was further demonstrated by assaying As^{III} and As^{V} in certified reference water (GBW08605, 500 μg kg^{-1} As^{III}), spiked lake water, and groundwater samples. For all the samples with As^{III} and As^{V} concentration over 7.5 μg L^{-1}, positive response was observed by naked eyes. In addition, the As^{III} and As^{V} concentration (μg L^{-1}) assayed by the proposed procedure with UV–vis detection agreed well with that by HPLC-AFS for the certified reference water, the groundwater and the spiked lake water. Results in Table 2 suggested the potential application of the proposed method for speciation test of As^{III} and As^{V} in real water samples.

Table 2. As^{III} and As^{V} Concentrations (μg L^{-1}, mean ± SD, n = 3) in Water Samples Determined by the Proposed Procedure (data obtained by UV–vis spectrophotometer) and Validated by HPLC-HG-AFS

	referred/spiked		detected[b]	
	As^{III}	As^{V}	As^{III}	As^{V}
lake water	15	15	16.5 ± 1.3	17.3 ± 1.5
underground water	256 ± 16[a]	390 ± 20[a]	270 ± 16	420 ± 44
certified reference water	450 ± 20[a]	N.D.[c]	462 ± 15	N.D.

[a]By the proposed procedure. [b]By HPLC-HG-AFS. [c]N.D.: lower than LOD (7.5 μg L^{-1}).

■ CONCLUSIONS

The selective interaction between $C_{14}(C_6)_3P^+$ and As^{III} was first demonstrated by EXAFS analysis. With the P-IL we have developed a sensitive As^{III}-specific P-AuNP probe for visual speciation test of As^{III} and As^{V} at levels below the WHO guideline for drinking water (10 μg L^{-1}). The extremely high specificity of the probe is attributed to the ILs modifier $C_{14}(C_6)_3P^+$, which has much stronger binding to As^{III} than As^{V}. The proposed probe also featured with low-cost, high tolerance to common coexisting ions such as 10 mM PO$_4^{3-}$, and no requirement of equipment, which make the probe suitable for field test of As^{III} and As^{V} in environmental waters. The excellent designability and the large pool of over 10^{18} kinds of ILs[54] provide great possibility in designing/selecting of task-specific ILs as coatings for preparation of AuNP probe, and our work opens a new window for the development of highly specific nanoparticle-based probes by selecting/designing proper ILs as modifiers.

■ ASSOCIATED CONTENT

Ⓢ Supporting Information

Transmission electron microscope (TEM) image of phosphonium ionic liquid-functionalized gold nanoparticles (P-AuNPs), transformation percentage of As^{III} along with the time in the presence and absence of P-AuNPs, effects of temperature and incubation time on the absorption ratio change, and interference evaluation in the presence of ascorbic acid. Supplemental figures are available free of charge via the Internet at http://pubs.acs.org.

■ AUTHOR INFORMATION

Corresponding Author

*E-mail: jfliu@rcees.ac.cn.

Notes

The authors declare no competing financial interest.

■ ACKNOWLEDGMENTS

This work was supported by the Strategic Priority Research Program of the Chinese Academy of Sciences (XDB14020101), the National Natural Science Foundation of China (21207124, 21025729), and the China Postdoctoral Science Foundation (2013T60181).

■ REFERENCES

(1) Shen, S. W.; Li, X. F.; Cullen, W. R.; Weinfeld, M.; Le, X. C. Arsenic Binding to Proteins. *Chem. Rev.* **2013**, *113*, 7769−7792.

(2) Mo, J. Y.; Xia, Y. J.; Wade, T. J.; Schmitt, M.; Le, X. C.; Dang, R. H.; Mumford, J. L. Chronic Arsenic Exposure and Oxidative Stress: OGG1 Expression and Arsenic Exposure, Nail Selenium, and Skin Hyperkeratosis in Inner Mongolia. *Environ. Health Perspect.* **2006**, *114*, 835−841.

(3) Aposhian, H. V. Enzymatic Methylation of Arsenic Species and Other New Approaches to Arsenic Toxicity. *Annu. Rev. Pharmacol. Toxicol.* **1997**, *37*, 397−419.

(4) Ravenscroft, P.; Brammer, H.; Richards, K. *Arsenic Pollution: a Global Synthesis*; Wiley: Chichester, U.K., 2009; pp 500.

(5) Fendorf, S.; Michael, H. A.; van Geen, A. Spatial and Temporal Variations of Groundwater Arsenic in South and Southeast Asia. *Science* **2010**, *328*, 1123−1127.

(6) Reeder, R. J.; Schoone, M. A. A.; Lanzirotti, A. Metal Speciation and Its Role in Bioaccessibility and Bioavailability. *Rev. Mineral. Geochem.* **2006**, *64*, 99−113.

(7) Sengupta, M. K.; Dasgupta, P. K. An Automated Hydride Generation Interface to ICPMS for Measuring Total Arsenic in Environmental Samples. *Anal. Chem.* **2009**, *81*, 9737−9743.

(8) Brown, R. J. C.; Yardley, R. E.; Brown, A. S.; Milton, M. J. T. Sample Matrix and Critical Interference Effects on the Recovery and Accuracy of Concentration Measurements of Arsenic in Ambient Particulate Samples Using ICP-MS. *J. Anal. At. Spectrom.* **2004**, *19*, 703−705.

(9) Cai, Y. Speciation and Analysis of Mercury, Arsenic, and Selenium by Atomic Fluorescence Spectrometry. *TrAC, Trends Anal. Chem.* **2000**, *19*, 62−66.

(10) Lu, Y. K.; Sun, H. W.; Yuan, C. G.; Yan, X. P. Simultaneous Determination of Trace Cadmium and Arsenic in Biological Samples by Hydride Generation-Double Channel Atomic Fluorescence Spectrometry. *Anal. Chem.* **2002**, *74*, 1525−1529.

(11) Rupasinghe, T.; Cardwell, T. J.; Cattrall, R. W.; de Castro, M. D. L.; Kolev, S. D. Pervaporation-Flow Injection Determination of Arsenic Based on Hydride Generation and the Molybdenum Blue Reaction. *Anal. Chim. Acta* **2001**, *445*, 229−238.

(12) Toda, K.; Ohba, T.; Takaki, M.; Karthikeyan, S.; Hirata, S.; Dasgupta, P. K. Speciation-Capable Field Instrument for the Measurement of Arsenite and Arsenate in Water. *Anal. Chem.* **2005**, *77*, 4765−4773.

(13) Morita, K.; Kaneko, E. Spectrophotometric Determination of Trace Arsenic in Water Samples Using a Nanoparticle of Ethyl Violet with a Molybdate-Iodine Tetrachloride Complex as a Probe for Molybdoarsenate. *Anal. Chem.* **2006**, *78*, 7682−7688.

(14) Siegfried, K.; Endes, C.; Bhuiyan, A. F. M. K.; Kuppardt, A.; Mattusch, J.; van der Meer, J. R.; Chatzinotas, A.; Harms, H. Field Testing of Arsenic in Groundwater Samples of Bangladesh Using a Test Kit Based on Lyophilized Bioreporter Bacteria. *Environ. Sci. Technol.* **2012**, *46*, 3281−3287.

(15) George, C. M.; Zheng, Y.; Graziano, J. H.; Rasul, S. B.; Hossain, Z.; Mey, J. L.; van Geen, A. Evaluation of an Arsenic Test Kit for Rapid Well Screening in Bangladesh. *Environ. Sci. Technol.* **2012**, *46*, 11213−11219.

(16) Biswas, A.; Nath, B.; Bhattacharya, P.; Halder, D.; Kundu, A. K.; Mandal, U.; Mukherjee, A.; Chatterjee, D.; Jacks, G. Testing Tubewell Platform Color as a Rapid Screening Tool for Arsenic and Manganese in Drinking Water Wells. *Environ. Sci. Technol.* **2012**, *46*, 434−440.

(17) Daniel, M. C.; Astruc, D. Gold nanoparticles: Assembly, Supramolecular Chemistry, Quantum-Size-Related Properties, and Applications toward Biology, Catalysis, and Nanotechnology. *Chem. Rev.* **2004**, *104*, 293−346.

(18) Ghosh, S. K.; Pal, T. Interparticle Coupling Effect on the Surface Plasmon Resonance of Gold Nanoparticles: From Theory to Applications. *Chem. Rev.* **2007**, *107*, 4797−4862.

(19) Ray, P. C. Size and Shape Dependent Second Order Nonlinear Optical Properties of Nanomaterials and Their Application in Biological and Chemical Sensing. *Chem. Rev.* **2010**, *110*, 5332−5365.

(20) Lee, J. S.; Han, M. S.; Mirkin, C. A. Colorimetric Detection of Mercuric Ion (Hg^{2+}) in Aqueous Media using DNA-Functionalized Gold Nanoparticles. *Angew. Chem., Int. Ed.* **2007**, *46*, 4093−4096.

(21) Tan, Z. Q.; Liu, J. F.; Jiang, G. B. Visual Test of Subparts Per Billion-Level Copper(II) by Fe_3O_4 Magnetic Nanoparticle-Based Solid Phase Extraction Coupled with a Functionalized Gold Nanoparticle Probe. *Nanoscale* **2012**, *4*, 6735−6738.

(22) Wilson, R. The Use of Gold Nanoparticles in Diagnostics and Detection. *Chem. Soc. Rev.* **2008**, *37*, 2028−2045.

(23) Liu, D. B.; Wang, Z.; Jiang, X. Y. Gold Nanoparticles for the Colorimetric and Fluorescent Detection of Ions and Small Organic Molecules. *Nanoscale* **2011**, *3*, 1421−1433.

(24) Huang, C. C.; Chang, H. T. Parameters for Selective Colorimetric Sensing of Mercury(II) in Aqueous Solutions Using Mercaptopropionic Acid-Modified Gold Nanoparticles. *Chem. Commun.* **2007**, *12*, 1215−1217.

(25) Darbha, G. K.; Singh, A. K.; Rai, U. S.; Yu, E.; Yu, H. T.; Ray, P. C. Selective Detection of Mercury (II) Ion Using Nonlinear Optical Properties of Gold Nanoparticles. *J. Am. Chem. Soc.* **2008**, *130*, 8038−8043.

(26) Xu, X. W.; Wang, J.; Jiao, K.; Yang, X. R. Colorimetric Detection of Mercury Ion (Hg^{2+}) Based on DNA Oligonucleotides and Unmodified Gold Nanoparticles Sensing System with a Tunable Detection Range. *Biosens. Bioelectron.* **2009**, *24*, 3153−3158.

(27) Tan, Z. Q.; Liu, J. F.; Liu, R.; Yin, Y. G.; Jiang, G. B. Visual and Colorimetric Detection of Hg^{2+} by Cloud Point Extraction with Functionalized Gold Nanoparticles as a Probe. *Chem. Commun.* **2009**, *45*, 7030−7032.

(28) Lin, C. Y.; Yu, C. J.; Lin, Y. H.; Tseng, W. L. Colorimetric Sensing of Silver(I) and Mercury(II) Ions Based on an Assembly of Tween 20-Stabilized Gold Nanoparticles. *Anal. Chem.* **2010**, *82*, 6830−6837.

(29) Liu, D. B.; Qu, W. S.; Chen, W. W.; Zhang, W.; Wang, Z.; Jiang, X. Y. Highly Sensitive, Colorimetric Detection of Mercury(II) in

Aqueous Media by Quaternary Ammonium Group-Capped Gold Nanoparticles at Room Temperature. *Anal. Chem.* **2010**, *82*, 9606–9610.

(30) Tan, Z. Q.; Liu, J. F. Visual Test of Subparts per Billion-Level Mercuric Ion with a Gold Nanoparticle Probe after Preconcentration by Hollow Fiber Supported Liquid Membrane. *Anal. Chem.* **2010**, *82*, 4222–4228.

(31) Du, J. J.; Jiang, L.; Shao, Q.; Liu, X. G.; Marks, R. S.; Ma, J.; Chen, X. D. Colorimetric Detection of Mercury Ions Based on Plasmonic Nanoparticles. *Small* **2013**, *9*, 1467–1481.

(32) Kalluri, J. R.; Arbneshi, T.; Khan, S. A.; Neely, A.; Candice, P.; Varisli, B.; Washington, M.; McAfee, S.; Robinson, B.; Banerjee, S.; et al. Use of Gold Nanoparticles in a Simple Colorimetric and Ultrasensitive Dynamic Light Scattering Assay: Selective Detection of Arsenic in Groundwater. *Angew. Chem., Int. Ed.* **2009**, *48*, 9668–9671.

(33) Wu, Y. G.; Zhan, S. S.; Wang, F. Z.; He, L.; Zhi, W. T.; Zhou, P. Cationic Polymers and Aptamers Mediated Aggregation of Gold Nanoparticles for the Colorimetric Detection of Arsenic(III) in Aqueous Solution. *Chem. Commun.* **2012**, *48*, 4459–4461.

(34) Luo, T.; Hu, S.; Cui, J. L.; Tian, H. X.; Jing, C. Y. Comparison of Arsenic Geochemical Evolution in the Datong Basin (Shanxi) and Hetao Basin (Inner Mongolia), China. *Appl. Geochme.* **2012**, *27*, 2315–2323.

(35) Itoh, H.; Naka, K.; Chujo, Y. Synthesis of Gold Nanoparticles Modified with Ionic Liquid Based on the Imidazolium Cation. *J. Am. Chem. Soc.* **2004**, *126*, 3026–3027.

(36) Ballinas, M. D.; Miguel, E. R. D.; Munoz, M.; de Gyves, J. Arsenic(V) Extraction from Sulfuric Acid Media Using DBBP-D2EHPA Organic Mixtures. *Ind. Eng. Chem. Res.* **2003**, *42*, 574–581.

(37) Hylton, K.; Mitra, S. A Microfluidic Hollow Fiber Membrane Extractor for Arsenic(V) Detection. *Anal. Chim. Acta* **2008**, *607*, 45–49.

(38) Perez, M. E. M.; Reyes-Aguilera, J. A.; Saucedo, T. I.; Gonzalez, M. P.; Navarro, R.; Avila-Rodriguez, M. Study of As(V) Transfer through a Supported Liquid Membrane Impregnated with Trioctylphosphine Oxide (Cyanex 921). *J. Membr. Sci.* **2007**, *302*, 119–126.

(39) Ballinas, M. D.; de San Miguel, E. R.; Rodriguez, M. T. D.; Silva, O.; Munoz, M.; de Gyves, J. Arsenic(V) Removal with Polymer Inclusion Membranes from Sulfuric Acid Media Using DBBP as Carrier. *Environ. Sci. Technol.* **2004**, *38*, 886–889.

(40) Monasterio, R. P.; Wuilloud, R. G. Ionic Liquid as Ion-Pairing Reagent for Liquid-Liquid Microextraction and Preconcentration of Arsenic Species in Natural Waters Followed by ETAAS. *J. Anal. At. Spectrom.* **2010**, *25*, 1485–1490.

(41) Duarte, G.; Ciminelli, V. S. T.; Dantas, M. S. S.; Duarte, H. A.; Vasconcelos, I. F.; Oliveira, A. F.; Osseo-Asare, K. As(III) Immobilization on Gibbsite: Investigation of the Complexation Mechanism by Combining EXAFS Analyses and DFT Calculations. *Geochim. Cosmochim. Acta* **2012**, *83*, 205–216.

(42) Luo, T.; Cui, J. L.; Hu, S.; Huang, Y. Y.; Jing, C. Y. Arsenic Removal and Recovery from Copper Smelting Wastewater Using TiO_2. *Environ. Sci. Technol.* **2010**, *44*, 9094–9098.

(43) Liu, J. F.; Jönsson, J. Å.; Jiang, G. B. Application of Ionic Liquids in Analytical Chemistry. *TrAC, Trends Anal. Chem.* **2005**, *24*, 20–27.

(44) Soukup-Hein, R. J.; Warnke, M. M.; Armstrong, D. W. Ionic Liquids in Analytical Chemistry. *Annu. Rev. Anal. Chem.* **2009**, *2*, 145–168.

(45) Hallett, J. P.; Welton, T. Room-Temperature Ionic Liquids: Solvents for Synthesis and Catalysis. 2. *Chem. Rev.* **2011**, *111*, 3508–3576.

(46) Liu, J. F.; Liu, R.; Yin, Y. G.; Jiang, G. B. Triton X-114 Based Cloud Point Extraction: a Thermoreversible Approach for Separation/Concentration and Dispersion of Nanomaterials in the Aqueous Phase. *Chem. Commun.* **2009**, *45*, 1514–1516.

(47) Xu, H.; Allard, B.; Grimvall, A. Effects of Acidification and Natural Organic Materials on the Mobility of Arsenic in the Environment. *Water Air Soil Poll.* **1991**, *57–58*, 269–278.

(48) Swedlund, P. J.; Webster, J. G. Adsorption and Polymerisation of Silicic Acid on Ferrihydrite, and Its Effect on Arsenic Adsorption. *Water Res.* **1999**, *33*, 3413–3422.

(49) Wang, S. L.; Mulligan, C. N. Effect of Natural Organic Matter on Arsenic Release from Soils and Sediments into Groundwater. *Environ. Geochem. Health.* **2006**, *28*, 197–214.

(50) Alguacil, F. J.; Alonso, M.; Lopez, F. A.; Lopez-Delgado, A. Pseudo-Emulsion Membrane Strip Dispersion (PEMSD) Pertraction of Chromium(VI) Using CYPHOS IL101 Ionic Liquid as Carrier. *Environ. Sci. Technol.* **2010**, *44*, 7504–7508.

(51) Leontidis, E. Hofmeister Anion Effects on Surfactant self-Assembly and the Formation of Mesoporous Solids. *Curr. Opin. Colloid Interface Sci.* **2002**, *7*, 81–91.

(52) Matsubara, C.; Yamamoto, Y.; Takamura, K. Rapid-Determination of Trace Amounts of Phosphate and Arsenate in Water by Spectrophotometric Detection of Their Heteropoly Acid-Malachite Green Aggregates Following Preconcentration by Membrane Filtration. *Analyst* **1987**, *112*, 1257–1260.

(53) Johnson, D. L. Simultaneous Determination of Arsenate and Phosphate in Natural Waters. *Environ. Sci. Technol.* **1971**, *5*, 411–414.

(54) Visser, A. E.; Swatloski, R. P.; Reichert, W. M.; Mayton, R.; Sheff, S.; Wierzbicki, A.; Davis, J. H.; Rogers, R. D. Task-Specific Ionic Liquids Incorporating Novel Cations for the Coordination and Extraction of Hg^{2+} and Cd^{2+}: Synthesis, Characterization, and Extraction Studies. *Environ. Sci. Technol.* **2002**, *36*, 2523–2529.